

Conventional and unconventional orderings in the jarosites

A. S. Wills*

Département de Recherche Fondamentale sur la Matière Condensée, SPSMS, CEA Grenoble, 38054 Grenoble, France.
(February 1, 2008)

The jarosites make up the most studied family of *kagomé* antiferromagnets. The flexibility of the structure to substitution of the A and B ions allows a wide range of compositions to be synthesised with the general formula $AB_3(SO_4)_2(OH)_6$ ($A = Na^+, K^+, Ag^+, Rb^+, H_3O^+, NH_4^+, \frac{1}{2}Ba^{2+}$, and $\frac{1}{2}Pb^{2+}$; $B = Fe^{3+}, Cr^{3+}$, and V^{3+}). Additional chemical tuning of the exchange between layers is also possible by substitution of the $(SO_4)^{2-}$ groups by $(SeO_4)^{2-}$ or $(CrO_4)^{2-}$. Thus, a variety of $S = 5/2, 3/2$, and 1 systems can be engineered to allow study of the effects of frustration in both the classical and more quantum limits. Within this family both conventional long-ranged magnetic order and more exotic unconventional orderings have been found. This article reviews the different types of magnetic orderings that occur and examines some of the parameters that are their cause.

PACS numbers: 75.25.+z, 75.30.Et, 75.30.Gw, 75.50.Ee, 75.50.Lk.

I. INTRODUCTION.

Research in frustrated magnetic systems follows two main directions. In the first, the effects of frustration are studied in systems that show otherwise conventional behaviour. Rather than being simply a study of the ‘soft modes’ that are characteristic of frustrated magnetism, these investigations can reveal fundamental differences in magnetic properties and their causes. The other, and frequently more pursued, direction is the search for, and study of, new and unconventional types of magnetic ground states. Particular effort in the study of frustrated magnetism is made on systems where the magnetic ions make up the *kagomé* and *pyrochlore* geometries. This is because the frustration of their triangular motifs is amplified by the vertex sharing topology, and is at such a degree that the conventional Néel -type of long-range order is not expected to occur even at $T = 0$ in the $S = \frac{1}{2}$ nearest-neighbour systems.

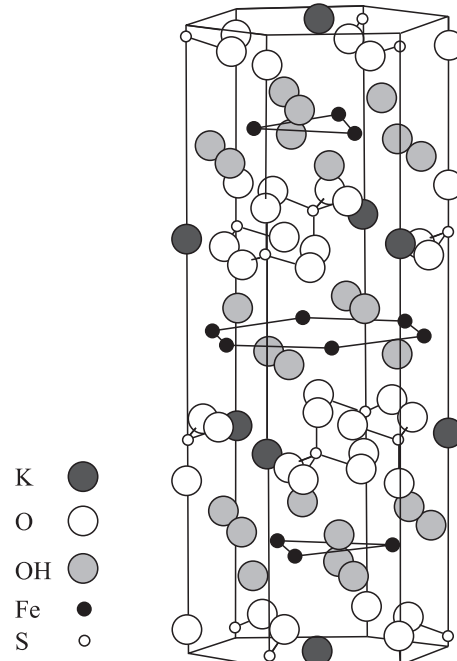
In this article a review is made of the observed magnetic properties of different members of the jarosite family. These present examples of systems in which the *kagomé* lattice of magnetic ions can be decorated by ions with a variety of spin states. They therefore provide access to the effects of frustration in classical and more quantum regimes, as evidenced in the low-temperature properties of both the members that possess long-ranged spin structures, and of those that show more unconventional orderings (Table I).

II. THE ALUNITE AND JAROSITE FAMILIES

In mineralogical terms, the jarosites are a subfamily of the alunite group. This is a series of compositions with the formula $AB_3(SO_4)_2(OH)_6$ (where $A = Na^+, K^+, Ag^+, Rb^+, H_3O^+, NH_4^+, \frac{1}{2}Ba^{2+}$, and $\frac{1}{2}Pb^{2+}$; and $B=Al^{3+}$ and Fe^{3+}); alunite itself has the formula

$KAl_3(SO_4)_2(OH)_6$.¹⁵ While in mineralogy the jarosites are the Fe members of this series, the term has been expanded by physicists to include the magnetic members of this series, *i.e.* those where $B=Fe^{3+}, Cr^{3+}$ and V^{3+} .¹¹⁻¹³ Thus, within the jarosites series the spin states can be tailored by chemical methods. Diamagnetic dilution studies can also be made in which a non-magnetic ion, such as Al^{3+}, Ga^{3+} , or In^{3+} , is substituted onto the B site.^{16,11} In addition to this versatility in engineering various *kagomé* systems, control can also be exercised over the details of the interplane magnetic exchange by replacement of the SO_4^{2-} ion by CrO_4^{2-} , or SeO_4^{2-} .¹⁶

FIG. 1. The crystal structure of jarosite, $KFe_3(SO_4)_2(OH)_6$.



III. CRYSTAL STRUCTURE.

The crystal structure of the majority of the jarosites is depicted in Figure 1.¹⁷ While there has been discussion over whether the actual space group is $R\bar{3}m$ or $R\bar{3}m$, the latter is now the generally accepted symmetry. A notable exception to this is $Pb_{0.5}Fe_3(SO_4)_2(OH)_6$, where segregation of the Pb^{2+} ions into mostly full and empty layers leads to a doubling of the unit cell along the c -direction.¹⁸ However, no other deviation away from the rhombohedral jarosite structure is shown in this material.

The most important features for the magnetic properties are the three *kagomé* layers of Fe^{3+} ions with the hexagonal stacking sequence ...ABC... The details of the intraplane and the interplane exchange will be examined separately in Sections IV A and IV B.

IV. FE COORDINATION AND EXCHANGE PATHWAYS

The magnetic Fe^{3+} ions are coordinated by a distorted octahedron made up of 4 equatorial hydroxy and 2 axial sulfate group oxygens, as shown in Figure 2: selected bond distances and angles are given in Table II. The octahedra are tilted with respect to the crystallographic c -direction, and it is this canting that defines the axis of any Ising single-ion anisotropy for the B^{3+} atoms. XY anisotropy is similarly defined by the plane of the 4 hydroxy groups.

A. Intralayer coupling

As shown in Figure 2, simple distance arguments indicate the strongest intralayer superexchange between nearest-neighbour B atoms is a pairwise interaction that takes place via a shared hydroxide group with a bridging angle of close to 133° . Unfortunately, the complexity of the superexchange at a non-linear or non-orthogonal angle prevents an explanation from being made of the exchange observed in these systems.

Also possible is exchange via the sulfate group (labelled S in the Figure). This is likely to be far weaker than that mediated by the bridging hydroxy group because it involves a greater number of chemical bonds. In the jarosite structure this sulfate is shared in the same way between the three B octahedra of a *kagomé* triangle, and so it will act to equally couple the three magnetic atoms of the triangle.

B. Interlayer coupling

The expectation that the jarosites could be tailored into providing good model *kagomé* systems comes from the large separation of the *kagomé* planes, with respect

to those within the plane: in $(H_3O)Fe_3(SO_4)_2(OH)_6$ the nearest neighbour B—B distance 3.66 \AA , whereas the distance between the *kagomé* layers is 5.94 \AA . The exchange between the *kagomé* layers is therefore anticipated to be far weaker than that within a layer from simple arguments of distance and the number of chemical bonds involved in the superexchange (Figure 4). Despite its relative weakness, it is apparent from the different propagation vectors observed in $KFe_3(SO_4)_2(OH)_6$ and $KFe_3(CrO_4)_2(OH)_6$ that the interlayer coupling involving the XO_4 ion plays a definitive rôle in the observed magnetic structure.

In a recent work, symmetry analysis has been used to determine the stability conditions of the different magnetic structures observed in the jarosites.¹⁴ In terms of an exchange constant relating the nearest B^{3+} atoms of neighbouring layers, it has been found that the different $\mathbf{k} = 00\frac{3}{2}$ spin configurations observed in $KFe_3(SO_4)_2(OD)_6$ ^{5,6} and $(H_3O)V_3(SO_4)_2(OH)_6$ ¹⁴ are stabilised by ferromagnetic and antiferromagnetic exchange respectively, while the $\mathbf{k} = 000$ spin structure observed in both $KCr_3(SO_4)_2(OD)_6$ ¹² and $KFe_3(CrO_4)_2(OD)_6$ ¹¹ is stabilised by antiferromagnetic coupling.

FIG. 2. The distorted octahedral coordination of the B^{3+} atoms, and their connection via a shared hydroxy oxygen. The third coordination octahedron has not been highlighted for clarity. Definitions of atom labels are made for Table II.

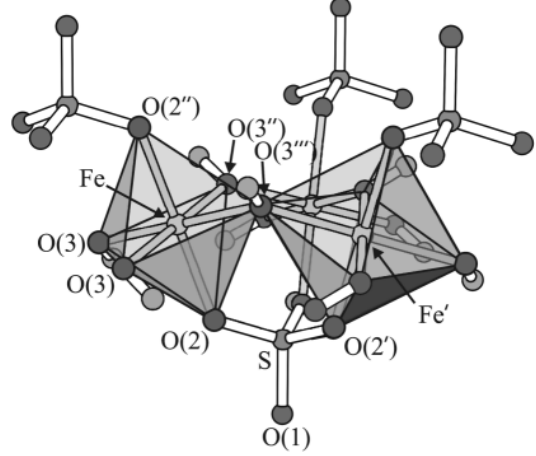
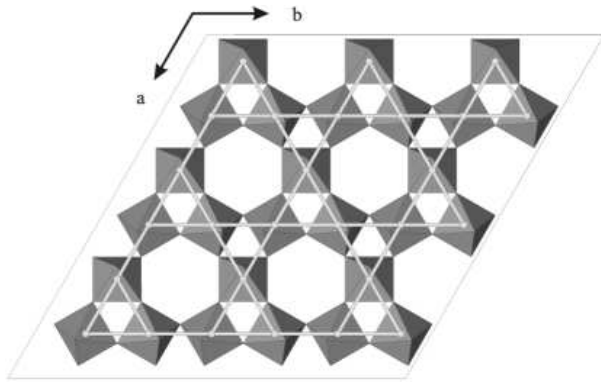


FIG. 3. The linkage of the distorted coordination octahedra around the B^{3+} to form the *kagomé* lattice.



C. Effects of A cation

The marked difference in the responses of hydronium jarosite from the other iron jarosites^{8,9,4} indicates that the A cation is capable of having a profound influence on the low-temperature magnetic properties of these systems. This is most likely a consequence of the non-spherical symmetry of the H_3O^+ ion and its ability to hydrogen bond with some of the 12 sulfate group oxygens that coordinate the A site. When the H_3O ions are no longer orientationally mobile, as is the situation at low temperature, these hydrogen bonds will create interactions between neighbouring sulfate groups that are not present in the other jarosites. Due to the complexity this would generate, it is not yet clear if they will act to hinder or improve the interlayer exchange. However, the large difference in the magnetic properties of the hydronium jarosite from those of the monatomic ions, even for compositions with the same Fe atom occupation,⁶ suggests that there is indeed a disruption of simple interlayer exchange couplings, and concomitantly a destabilisation of any long-range ordered state that they would induce.

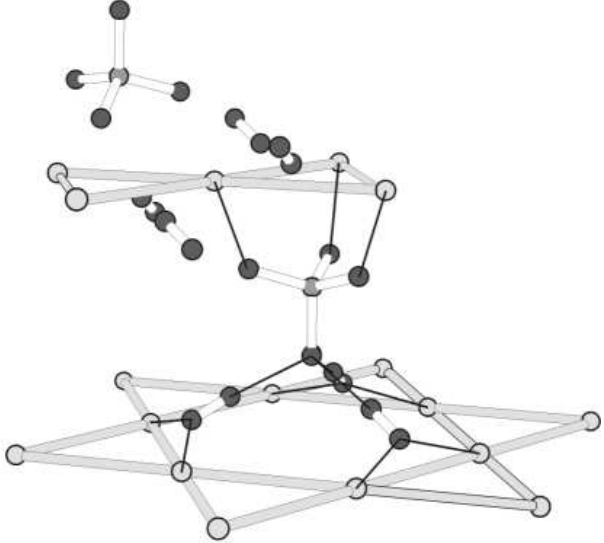
That the ammonium salt⁴ behaves like the other spherical A-site metals, suggests that its hydrogen bonding is either less disturbing, or of a lesser consequence, than that of H_3O . Further studies are required before the effects of the A cation can be understood.

V. INFLUENCES OF NONSTOICHIOMETRY.

It is well known that the jarosites are subject to non-stoichiometry on both the A and the B sites. Deficiency of the A metal or ammonium cation is charge compensated for by incorporation of H_3O^+ ions onto the A site, so that the site occupation remains essentially at unity.¹⁹ The extreme limit of this situation is of course the hydronium salt itself. Under-occupation of the B site results in protonation of the hydroxy groups in the structure. As these groups play the dominant rôle in the mediation of the superexchange between the metal centres, it is conceivable that such disorder and the associated random-

ness in the exchange interactions, could have important consequences for the magnetic properties.

FIG. 4. Exchange paths between the *kagomé* layers in the jarosite structure.



VI. CONVENTIONAL ORDERINGS

Long-range magnetic structures with the propagation vectors* $\mathbf{k} = 000$ and $\mathbf{k} = 00\frac{3}{2}$ have been observed in the jarosites (see Table I). Representational Analysis calculations have shown that there are only 3 non-zero irreducible representations for the 9d B^{3+} site and that the basis vectors associated with them are identical for both values of the propagation vector; they are shown in Figure 5.¹⁴ These calculations show that for both of these values of \mathbf{k} , the same inplane spin configurations are allowed, and that the relation between moments in successive *kagomé* layers is determined simply by the value of \mathbf{k} : in the case of $\mathbf{k}=0$, the moments related by unit translations of the primitive cell are ferromagnetically aligned, while those for $\mathbf{k} = 00\frac{3}{2}$ are antiferromagnetically aligned.

The basis vectors for the unrepeated first order irreducible representation, here labelled Γ_1 , correspond to a 120° structure in which the moments are fixed along particular crystallographic axes. Those of the doubly-repeated irreducible representation, Γ_3 , form an umbrella structure made up of a 120° configuration, in which the in-plane component of the spins are related by 60° to those of Γ_1 , and a ferromagnetic component along the crystallographic *c*-axis.

*both propagation vectors and Wyckoff labels refer to the non-primitive hexagonal setting of $\bar{R}\bar{3}\text{m}$

It is notable that both these 120° structures possess a uniform chirality, $\kappa = +1$. Where κ is defined as the pairwise vector product clockwise around a triangle:

$$\kappa = \frac{2}{(3\sqrt{3})} [\mathbf{S}_1 \times \mathbf{S}_2 + \mathbf{S}_2 \times \mathbf{S}_3 + \mathbf{S}_3 \times \mathbf{S}_1], \quad (1)$$

Thus, it is a consequence of symmetry, rather than anisotropy⁵, that the $q = 0$ spin configurations with $\kappa = -1$ are forbidden.

The third irreducible representation, Γ_6 , is 2 dimensional and is repeated 3 times. This leads to a total of 6 basis vectors which describe in general a complex spin configuration. However, conjugate pairing on these basis vectors leads to only 3 being required to describe all the possible orderings under this irreducible representation. Notably, coplanar ordering under this representation involves non-spin compensated triangles, *i.e.*

$$\sum_i \mathbf{S} \neq 0 \quad (2)$$

Where the sum is over the moments of an individual triangle. There is therefore a net moment associated with each of the *kagomé* planes.

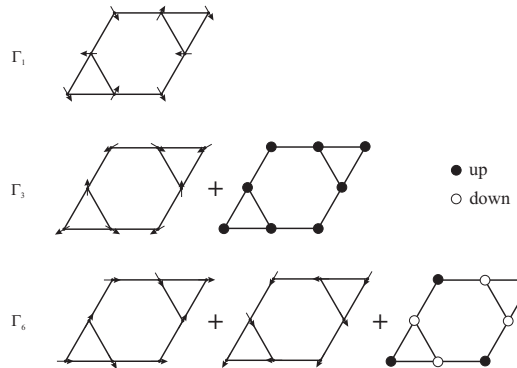


FIG. 5. The motifs for the different basis vectors for the non-zero irreducible representations of the point group D_{3d}^5 at the B site for the propagation vectors $\mathbf{k}=0$ and $\mathbf{k}=00\frac{3}{2}$. The labelling scheme follows that for $\mathbf{k}=0$.¹⁴

A. $\mathbf{k} = 000$

Magnetic ordering with the magnetic cell the same size as the nuclear has been observed in the compositions $\text{KFe}_3(\text{CrO}_4)_2(\text{OD})_6$ ¹¹ and $\text{KCr}_3(\text{SO}_4)_2(\text{OD})_6$.^{11,12} In both cases it is believed that the nearest neighbour antiferromagnetic exchange results in a 120° spin structure, while some secondary interaction such a single-ion anisotropy leads to a small canting of the moments along the *c*-axis. The presence of such a ferromagnetic component in a system with antiferromagnetic nearest-neighbour interactions is compatible only with ordering under the repeated first-order representation, Γ_3 . The general structure may thus be described by an umbrella mode involving some linear combination of the two basis vectors.

B. $\mathbf{k} = 00\frac{3}{2}$

Ordering with this propagation vector is found in the majority of the iron jarosites ($\text{AFe}_3(\text{SO}_4)_2(\text{OD})_6$, where $\text{A} = \text{Na}^+$, K^+ , Ag^+ , Rb^+ , Tl^+ , H_3O^+ , and ND_4^+) and the vanadium salt $(\text{H}_3\text{O})\text{V}_3(\text{SO}_4)_2(\text{OH})_6$. In all the Fe compositions, ordering under the repeated first-order representation is again observed.¹⁴ Hydronium vanadium jarosite in contrast, shows ordering under the representation Γ_6 .¹⁴

At present there are still questions over the details of the ordering transitions in the iron jarosites as some samples exhibit two ordering transitions^{3,4,6} while others display only one.⁵ Recent refinement of neutron powder diffraction data collected from $\text{KFe}_3(\text{SO}_4)_2(\text{OD})_6$ have shown that in the samples with two transitions the intermediate phase is an umbrella structure based on Γ_3 . Muon Spin Relaxation (MuSR) experiments revealed the presence of large fluctuations in this intermediate structure that reduce the size of the ordered moment. Harrison *et al.*²⁰ confirmed the absence of an out-of-plane component to the ordering by single crystal neutron diffraction from a natural sample using the technique of spherical polarisation analysis, and demonstrated by powder neutron diffraction that the lower-temperature transition, in which the moments drop into the *kagomé* plane, is disrupted by disorder on the magnetic B sites.⁶ The display of a single transition is therefore likely to be consequence of sample nonstoichiometry. As the out-of-plane component of the intermediate phase is not stabilised by exchange interactions, it suggests the presence of some other influence, such as Ising single-ion anisotropy. It is however difficult to imagine that this anisotropy changes to being XY so close to the first ordering temperature (in $\text{KFe}_3(\text{SO}_4)_2(\text{OD})_6$, $T_{C1}=64.5$ K and $T_{C2}=57$ K), and the reasons for the second transition are consequentially still unclear.

The magnetic structure observed in $(\text{H}_3\text{O})\text{V}_3(\text{SO}_4)_2(\text{OH})_6$ will be discussed later in Section VII C as its origins appear to be unconventional.

VII. UNCONVENTIONAL ORDERINGS.

This section presents a brief review of the unconventional orderings observed in the jarosites as a function of the different spin values.

A. $S = \frac{5}{2}$ Topological Spin Glass.

The most studied member of the jarosite series is the hydronium salt $(\text{H}_3\text{O})\text{Fe}_3(\text{SO}_4)_2(\text{OH})_6$, which is an example of an unconventional spin glass.^{8,9,4,10} Before describing its responses, it is useful to examine the occurrence of glassy magnetic phases in geometrically frustrated antiferromagnets. In relation to the undercon-

strained lattices, this possibility was first studied by Villain²¹, who noted that the high degeneracy of the magnetic *pyrochlore* sublattice of the B-site of the spinels is robust to the introduction of a small degree of disorder. This conclusion can be trivially extended to the *kagomé* antiferromagnet, and so establishes that small amounts of disorder should not give rise to a spin glass phase. Villain further noted that if the degree of disorder was sufficient to break the degeneracies present in the system, then the spin glass-like state that would result would not necessarily be typical as the large degree of frustration in these systems could still lead to unconventional physics. There is therefore a question that hangs over any unconventional spin glass phases observed in the highly frustrated lattices: *are they the result of disorder in the sample, whether related to sites or bonding (exchange) ?*

With an occupation of the magnetic sublattice of $\sim 97\%$, the degree of site-disorder present in hydronium jarosites is not expected to be at the level required to stabilise spin glass behaviour.⁸ The vitreous magnetic phase observed at low temperature is ergo quite remarkable. Measurements of the thermodynamic and kinetic properties confirm its notability as they indicate clearly that the glassy magnetic phase seen below a critical transition at $T_g \sim 17\text{ K}$ ¹⁰ is unlike those of conventional site-disordered spin glasses²²: the magnetic contribution to the specific heat follows a T^2 relation with temperature,⁹ as opposed to the linear law typical of site-disordered systems, and the temperature dependence of the out-of-equilibrium dynamics is remarkably weak.¹⁰ The latter provides interesting information about the spin glass state itself: if the relaxation of a spin glass is envisaged as involving the movement towards some equilibrium value, these results indicate that this equilibrium state changes *far* slower with temperature in hydronium jarosite than in conventional spin glass systems, a situation that is intriguing reminiscent of a system moving through a highly degenerate ground state manifold.

Polarised neutron powder diffraction studies of $(\text{D}_3\text{O})\text{Fe}_3(\text{SO}_4)_2(\text{OD})_6$ have shown that despite a freezing temperature of $T_g \sim 17\text{ K}$, short-ranged correlations are present at temperatures as high as 250 K , demonstrating well the difficulty with which the moments are freezing.^{23,24} The depression of the freezing temperature with relation to the exchange energy is compatible with suggestions of the freezing being a consequence of a new energy scale—a reduced Kosterlitz-Thouless temperature—that approximates to $\theta/48$ for an XY system.^{25,26} The magnitude and spatial extension of the correlations increase only gradually with cooling, until they reach an apparent saturation value of $\sim 10\text{ \AA}$ at 1.5 K .

Another unorthodox feature of this unconventional spin glass state is its fragility. In sharp contrast with site-disordered spin glasses, where an increase in disorder has only a small effect on the magnetic properties, in hydronium jarosite a deliberate increase in the level of disorder to $\sim 10\%$ is found to induce long-range magnetic order.⁴

This is an example of ‘order-by-disorder’,^{27–29} where increased disorder acts to stabilise the formation of long-range Néel order with respect to a spin glass state.

While the question of the influences of disorder remains unanswered in $(\text{H}_3\text{O})\text{Fe}_3(\text{SO}_4)_2(\text{OH})_6$, the unconventional nature of the observed spin glass phase is manifest. It is clear that the origins of the spin glass state itself and these unconventional properties are related to the frustrated topology of the *kagomé* lattice. This has lead to hydronium jarosite being termed a *topological spin glass*.¹⁰

B. $S = \frac{3}{2}$ Highly Fluctuating Ground States.

The apparent nonconformity of the magnetic properties of the hydronium jarosites when compared with the other Fe jarosites holds true also for the chromium analogue. While $\text{KCr}_3(\text{SO}_4)_2(\text{OD})_6$ shows a transition to long-range order¹², albeit with a greatly reduced sublattice magnetisation, due to the presence of quantum fluctuations, hydronium chromium jarosite $(\text{H}_3\text{O})\text{Cr}_3(\text{SO}_4)_2(\text{OH})_6$ displays quite different behaviour.¹³ Despite strong antiferromagnetic exchange ($\theta \simeq -60\text{ K}$), at low temperatures only a broad feature corresponding to the onset of short-ranged correlations is observed at $\sim 30\text{ K}$ in the dc susceptibility, before a small ferromagnetic transition at 2.2 K . The ferromagnetic nature of the correlations involved in this transition is confirmed by the field-dependence of the specific heat data below $\sim 5\text{ K}$. The magnetic entropy associated with the low temperature transition is only 5.4% is the value expected for a $S = \frac{3}{2}$ system and suggests the presence of extensive quantum fluctuations.

C. $S = 1$ Unconventional long-range order.

The $S = 1$ *kagomé* system $(\text{H}_3\text{O})\text{V}_3(\text{SO}_4)_2(\text{OH})_6$ has been shown to possess long-range order below a critical transition of $T_C \simeq 20\text{ K}$.^{13,14} However, the magnetic structure observed is remarkable because despite the non-zero exchange field experienced by each moment, some are orientated such as to nullify their exchange energy.¹⁴ It therefore appears that simple arguments of the long-range order being the result of minimised exchange energy cannot explain the formation of this ground state configuration. Rather, recent work has suggested that it is the result of a particular combination of ferromagnetic nearest-neighbour exchange and Ising anisotropies. Notably, these are precisely the types required to stabilise a spin ice phase on the *kagomé* lattice.³⁰

the additional degeneracies that are afforded by these particular spin orientations appear to be the cause of their stabilisation.

VIII. DISCUSSION AND CONCLUSION

There are still numerous questions concerning the effects of nonstoichiometry and how substitution of the different ions influences the magnetic exchange in the jarosites. In particular, the reasons for the apparent distinction of the hydronium salts remains unclear. Unfortunately, these questions are difficult to answer experimentally because synthetic limitations require that the majority of experiments are carried out on powders. Inferences made from the materials that show more comprehensible long-range orderings are consequently important in aiding understanding of those that show more unconventional order. This is well exemplified by the apparent planar anisotropy at low temperature in $\text{KFe}_3(\text{SO}_4)_2(\text{OD})_6$. Its observation is important, as such an anisotropy is required by a theoretical model of an unconventional spin glass ground state on the *kagomé* antiferromagnet.^{25,26}

As this paper has shown, the members of the jarosite family display a wide variety of interesting physics. The unconventional spin glass, highly fluctuating, and unconventional long-range magnetic orderings show well different influences of frustration that are still far from being explained. It is hoped that this review will incite further work on these intriguing materials.

- ¹³ A. S. Wills, *Ph.D. Thesis*, The University of Edinburgh (1997)
- ¹⁴ A. S. Wills, Phys. Rev. B, **63**, 064430 (2001).
- ¹⁵ C. Palache, H. Berman, and C. Frondel, *Dana's system of mineralogy* (John Wiley and Sons, London, 1951).
- ¹⁶ J. E. Dutrizac, NATO Conf. Ser. (Hydrometall. Process. Fund.) (1984).
- ¹⁷ S. B. Hendricks, Am. Miner. **22**, 773 (1937).
- ¹⁸ J. T. Szymanski, Can. Miner. **23**, 659 (1985).
- ¹⁹ J. Kubisz, Miner. Pol. **1**, 45 (1970).
- ²⁰ E. Lelievre-Berna, A. Harrison, G. Oakley, and D. Visser, Annual Report of the Institute Laue Langevin for 1999 (2000) expt 5-61-37.
- ²¹ J. Villain, J. Phys. (Paris) **38**, 26 (1977).
- ²² J. A. Mydosh, *Spin glasses: an experimental introduction* (Taylor & Francis Ltd, London 1993).
- ²³ G. S. Oakley, D. Visser, J. Frunzke, K. H. Andersen, A. S. Wills, and A. Harrison, Physica B **267-268**, 142 (1999).
- ²⁴ A. S. Wills, G. S. Oakley, D. Visser, J. Frunzke, A. Harrison, and K. H. Andersen, Phys. Rev. B *in press* (2001).
- ²⁵ I. Ritchey, P. Chandra, and P. Coleman, Phys. Rev. B **47**, 15342 (1993).
- ²⁶ P. Chandra, P. Coleman, and I. Ritchey, J. Physique I **3**, 591 (1993).
- ²⁷ J. Villain, R. Bidaux, J.-P. Carton, and R. Conte, J. Physique **41**, 1263 (1980).
- ²⁸ J. N. Reimers, Phys. Rev. B **45**, 7287 (1992).
- ²⁹ J. T. Chalker, P. C. W. Holdsworth, and E. F. Shender, Phys. Rev. Lett. **68**, 855 (1992).
- ³⁰ A. S. Wills, R. Ballou, and C. Larcoix, *paper in preparation* (2001).

* Present address: Institut Laue-Langevin, 6 rue Jules Horowitz, BP 156, 38042 Grenoble Cedex 9, France.

¹ A. B. Harris, C. Kallin, and A. J. Berlinsky, Phys. Rev. B **45**, 2899 (1992).

² J. N. Reimers and A. J. Berlinsky, Phys. Rev. B **48**, 9539 (1993).

³ S. Maegawa, M. Nishiyama, N. Tanaka, A. Oyamada, and M. Takano, J. Phys. Soc. Jpn. **65**, 2776 (1996).

⁴ A. S. Wills, A. Harrison, C. Ritter, and R. I. Smith, Phys. Rev. B **61**, 6156 (2000).

⁵ T. Inami, M. Nishiyama, S. Maegawa, and Y. Oka, Phys. Rev. B **61**, 12181 (2000).

⁶ J. Frunzke, T. Hansen, A. Harrison, J. S. Lord, G. S. Oakley, D. Visser, and A. S. Wills, J. Mater. Chem. *In press* (2001).

⁷ M. F. Collins, *Unpublished work*.

⁸ A. S. Wills and A. Harrison, J. Chem. Soc. Faraday Trans. **92**, 2161 (1996).

⁹ A. S. Wills, A. Harrison, S. A. M. Mentink, T. E. Mason, and Z. Tun, Europhys. Lett. **42**, 325 (1998).

¹⁰ A. S. Wills, V. Depuis, E. Vincent and R. Calemczuk, Phys. Rev. B **62**, R9264 (2000).

¹¹ M. G. Townsend, G. Longworth, and E. Roudaut, Phys. Rev. B **33**, 4919 (1986).

¹² S.-H. Lee, C. Broholm, M. F. Collins, L. Heller, A. P. Ramirez, Ch. Kloc, E. Bucher, R. W. Erwin, and N. Lavecic, Phys. Rev. B **56**, 8091 (1997).

TABLE I. Values of the intercept of the inverse susceptibility with the temperature axis θ , the exchange constant J , the critical temperature T_C , and order types for various members of the family $AB_3(XO_4)_2(OH)_6$. As series expansion calculations^{1,2} indicate that a modified form of the Curie-Weiss law holds below $T \simeq JS(S+1)/k$, J is calculated from $\theta = -2JS(S+1)/k_B$ for the Fe jarosites, while the conventional mean field result $\theta = -(4/3k_B)JS(S+1)$ is used for the other compositions.

Formula	θ /K	J /K	T_C /K	Ordering type	Ref.
$NaFe_3(SO_4)_2(OH)_6$	-730	41.7	60, 54	$k = 00\frac{3}{2}$	³
$NaFe_3(SO_4)_2(OH)_6$	-667	38.1	62, 42	$k = 00\frac{3}{2}$	⁴
$KFe_3(SO_4)_2(OH)_6$	-700	40.0	65	$k = 00\frac{3}{2}$	⁵
$KFe_3(SO_4)_2(OH)_6$	-663	37.9	64.5, 57.0	$k = 00\frac{3}{2}$	⁶
$(NH_4)Fe_3(SO_4)_2(OH)_6$	-670	38.3	61.7, 57.1	$k = 00\frac{3}{2}$	³
$(ND_4)Fe_3(SO_4)_2(OD)_6$	-640	36.6	62, 46	$k = 00\frac{3}{2}$	⁴
$Pb_{0.5}Fe_3(SO_4)_2(OH)_6$	-	-	-	$k = 00\frac{3}{2}$	⁷
$TlFe_3(SO_4)_2(OH)_6$	-	-	-	$k = 00\frac{3}{2}$	⁷
$AgFe_3(SO_4)_2(OD)_6$	-677	38.7	51	$k = 00\frac{3}{2}$	⁴
$RbFe_3(SO_4)_2(OD)_6$	-688	39.3	47	$k = 00\frac{3}{2}$	⁴
$(D_3O)Fe_{3-x}Al_y(SO_4)_2(OD)_6$	-720	41.1	41.1	$k = 00\frac{3}{2}$	⁴
$(D_3O)Fe_3(SO_4)_2(OD)_6$	-700	40.0	13.8	unconventional spin glass	⁸⁻¹⁰
$KFe_3(CrO_4)_2(OH)_6$	-600	34.2	65	$k = 000$	¹¹
$KCr_3(SO_4)_2(OH)_6$	-70	14	1.6	$k = 000$	¹²
$(H_3O)Cr_3(SO_4)_2(OD)_6$	-78	15.6	1.2	unknown	¹³
$(H_3O)V_3(SO_4)_2(OD)_6$	-45	9	21	$k = 00\frac{3}{2}$	¹⁴

TABLE II. Selected bond lengths and angles for $(H_3O)Fe_3(SO_4)_2(OH)_6$ at 1.5 K.⁸

Bond	Bond length (Å)	Bond Angle (°)
Fe—Fe	3.66228 (6)	
Fe—O(2)	2.0374 (19)	
Fe—O(3)	1.9921(8)	
S—O(1)	1.492 (5)	
S—O(2)	1.4495 (26)	
O(2)—O(3)	2.8236 (15)	
O(2'')—O(3)	2.8750 (27)	
O(3)—O(3')	2.8103 (33)	
O(3')—O(3'')	2.8240 (20)	
O(2)—S—O(2')		110.83 (23)
O(2)—S—O(1)		108.08 (24)
S—O(2)—Fe		129.265 (8)
Fe—O(3)—Fe'		133.625 (1)
O(2)—Fe—O(3)		88.968 (13)
O(3)—Fe—O(3')		89.721 (13)
O(3')—Fe—O(3'')		90.279 (19)